

*Article*

## Low-temperature behaviour of social and economic networks

Diego Garlaschelli <sup>1,\*</sup>, Sebastian E. Ahnert <sup>2</sup>, Thomas M. A. Fink <sup>3</sup> and Guido Caldarelli <sup>4,3,5</sup><sup>1</sup> Lorentz Institute of Theoretical Physics, University of Leiden, Niels Bohrweg 2, 2333 CA Leiden, The Netherlands<sup>2</sup> Theory of Condensed Matter, Cavendish Laboratory, University of Cambridge, JJ Thomson Avenue, CB3 0HE Cambridge, United Kingdom<sup>3</sup> London Institute for Mathematical Sciences, 22 South Audley St, W1K 2NY London, United Kingdom<sup>4</sup> IMT Alti Studi Lucca, Piazza S. Ponziano 6, 55100 Lucca, Italy<sup>5</sup> ISC-CNR, Dipartimento di Fisica, Università La Sapienza, P.le A. Moro 2, 00185 Roma, Italy

\* Author to whom correspondence should be addressed; garlaschelli@lorentz.leidenuniv.nl

*Version September 8, 2021 submitted to Entropy. Typeset by L<sup>A</sup>T<sub>E</sub>X using class file mdpi.cls*

**Abstract:** Real-world social and economic networks typically display a number of particular topological properties, such as a giant connected component, a broad degree distribution, the small-world property and the presence of communities of densely interconnected nodes. Several models, including ensembles of networks also known in social science as Exponential Random Graphs, have been proposed with the aim of reproducing each of these properties in isolation. Here we define a generalized ensemble of graphs by introducing the concept of *graph temperature*, controlling the degree of topological optimization of a network. We consider the temperature-dependent version of both existing and novel models and show that all the aforementioned topological properties can be simultaneously understood as the natural outcomes of an optimized, low-temperature topology. We also show that seemingly different graph models, as well as techniques used to extract information from real networks, are all found to be particular low-temperature cases of the same generalized formalism. One such technique allows us to extend our approach to real weighted networks. Our results suggest that a low graph temperature might be an ubiquitous property of real socio-economic networks, placing conditions on the diffusion of information across these systems.

**Keywords:** Complex networks; graph ensembles; graph temperature**Classification:** PACS 89.75.Hc, 89.75.Fb, 05.70.-a

## 19 1. Introduction

20 Complex networks have attracted the interest of physicists because statistical physics has proven to be  
21 an effective tool for the measurement and explanation of robust empirical properties of these networks  
22 [1,2]. Social and economic networks in particular often exhibit particular topological properties such  
23 as the presence of a *giant connected component* (a set of mutually reachable vertices spanning a finite  
24 fraction of the system), the ‘*small-world*’ property (the combination of a large density of triangles and a  
25 short distance among nodes), *community structure* (a subdivision of the network into modules of densely  
26 interconnected nodes), and a *broad degree distribution* (the presence of many more highly connected  
27 vertices than expected in random graphs).

28 Taken together, these properties place conditions on the diffusion of information in social networks.  
29 For instance, the ‘*strength of weak ties*’ effect [3], i.e. the phenomenon by which links connecting  
30 different communities are sparser and weaker than intra-community links, implies that the dynamics  
31 of information is mostly confined within communities, with rare (but crucial in terms of network-wide  
32 communication) jumps across different communities. In combination with the ‘small-world’ property,  
33 this means that real social networks display what has been called the ‘*small but slow world*’ effect [4]:  
34 even if, at a purely topological level, it only takes a few steps to connect two randomly chosen nodes (that  
35 are in general found in different communities), these steps are not the ones taken by typical dynamical  
36 processes (which are instead confined within communities). The result is an overall slowing down of the  
37 dynamics.

38 Among the several approaches that have been explored in order to reproduce the structure of real  
39 social and economic networks, an interesting class of models has a long tradition in social network  
40 analysis and goes under the name of *Exponential Random Graphs* (ERGs) [5]. ERGs allow one to  
41 specify a set of desired topological properties or ‘constraints’, and estimate the probability to be assigned  
42 to every possible network in order to reproduce the observed values of such properties. More recently,  
43 ERGs have been shown to be equivalent to a class of statistical ensembles of graphs [6] and have been  
44 further generalized [7–15]. This powerful formalism allows one to treat in a unified fashion a large  
45 class of models, including random graphs [1,2], the Configuration Model [16], Hidden Variable models  
46 [17,18] and extensions of them [6,9]. If we restrict ourselves to binary networks with a fixed number of  
47 vertices  $N$  and with no self-loops or multiple edges, the analogy with statistical physics lies in the fact  
48 that in these models each link can be regarded as a ‘particle’ that can be placed between any two vertices,  
49 subject to the constraint that the ‘occupation number’ for each pair of vertices  $i, j$  can only be  $a_{ij} = 0, 1$   
50 (for missing or existing links respectively) as in the familiar Fermi statistics. Clearly,  $a_{ij}$  coincides with  
51 the entries of the  $N \times N$  adjacency matrix  $A$  characterizing the topology completely. Each allowed  
52 adjacency matrix  $A$  corresponds to a possible configuration, and the set of possible configurations (each  
53 with its statistical weight  $P_A$ ) defines the statistical ensemble of graphs. Thus, the framework of ERGs  
54 allows one to develop the ‘statistical mechanics of networks’ by exploiting a range of tools which are  
55 well known in physics [6].

56 A multitude of specifications of ERGs have been proposed in order to reproduce, mostly in isolation  
57 from each other, the topological properties mentioned above [7–15]. Here we show that, if the analogy  
58 with statistical physics is completed via the introduction of the concept of *graph temperature*, all the  
59 above empirical properties can be easily understood as the consequences of a single phenomenon:  
60 the fact that real networks tend to have a low value of the temperature, presumably as the result of a  
61 topological optimization driven by the cost of establishing links.

62 In particular we find that many well-known topological properties such as the presence of a giant  
63 component, a scale-free degree distribution, the small-world effect, and a modular or ‘community’  
64 structure can be easily understood in terms of the low-temperature behaviour of real networks.

## 65 2. Temperature-dependent ensembles of graphs

66 We will now generalize the existing statistical formalism in order to include the concept of graph  
67 temperature. To realize why this extension is important, we note that in all ERG models the probability  
68  $P_A$  depends on the *energy*  $E_A$ , representing the topological ‘cost’ of realising the particular graph  $A$ . The  
69 energy  $E_A$  is chosen to be a linear combination of the so-called ‘constraints’ [6,12], i.e. the topological  
70 quantities that one desires to enforce.

71 Now, the concept of topological cost, or energy, is unclear without the quantification of its  
72 relative role with respect to the available *resources* that can be exploited to form the network. The  
73 relative importance of ‘cost’ and ‘available resources’ is usually controlled in statistical physics by  
74 the temperature. The zero-temperature regime corresponds to complete optimization, so that only  
75 the cheapest configuration can be formed and the units of the system occupy the states with lowest  
76 energy (this is the *optimized* case). In the opposite, infinite-temperature extreme the system does not  
77 distinguish between energetically cheap and expensive states, so that all configurations occur with  
78 the same probability. The formalism that we develop here is particularly suitable to model networks  
79 subject to such economic/engineering constraints. We shall complement the standard results obtained  
80 in the literature for the generic finite-temperature case (which is recovered when  $T = 1$ ) with the  
81 interesting ones corresponding to zero and infinite temperature, which are not accessible to current  
82 finite-temperature models. We find that a range of interesting results can be obtained by even the simplest  
83 models when  $T$  is allowed to vary, in particular when  $T$  approaches zero.

84 Our approach works equally well for directed and undirected graphs, but for the sake of simplicity  
85 we write all the expressions for the undirected case only. The generalization to directed graphs is  
86 straightforward. Similarly, the full generalization to weighted networks is possible using the available  
87 results for weighted ensembles [10,12,13], but we will not consider it here. Rather, we will consider a  
88 partial generalization to weighted networks by exploiting one particular approach that we have recently  
89 proposed to relate edge weights to edge probabilities [19].

### 90 2.1. General formalism

The most general statistical ensemble for an equilibrium undirected network is a *grandcanonical* one  
with  $2^{N(N-1)/2}$  graphs having a fixed number of vertices  $N$  and a varying number of links  $L_A = \sum_{ij} a_{ij}$ ,  
controlled by the *chemical potential*  $\mu$  [6,9]. The chemical potential is an important parameter governing

the link density of the network and the probability of connections [9]. However, in order to have a global parameter coupled not only to the number of links, but also to any other topological property of the network, we also introduce the *graph temperature*  $T$ . We therefore define a generalized ensemble where the probability of graph  $A$  is given by

$$P_A = \frac{1}{\mathcal{Z}} \exp \left[ \frac{\mu L_A - E_A}{T} \right] \quad (1)$$

where  $E_A$  is the *energy* of the particular graph  $A$  (a function of one or more topological properties of  $A$ , to be specified in each particular model) and

$$\mathcal{Z} \equiv \sum_A \exp \left[ \frac{\mu L_A - E_A}{T} \right] \quad (2)$$

91 is the *grand partition function* of the ensemble. Note that when  $T \rightarrow \infty$  we have  $P_A = 2^{-N(N-1)/2}$  for  
 92 all graphs, while when  $T \rightarrow 0$  we have  $P_A = 1$  for the graph with the maximum value of  $\mu L_A - E_A$  (or  
 93  $P_A = M^{-1}$  if there are  $M$  degenerate such graphs), and  $P_A = 0$  for all other graphs.

94 The temperature in eq.(1) might appear to be redundant, since the parameter  $T$  can be in principle  
 95 reabsorbed in a redefinition of  $E_A$  and  $\mu$  without loss of generality. In other words, all choices of  
 96 parameters that lead to the same values of  $E_A/T$  and  $\mu/T$  will generate indistinguishable results,  
 97 meaning that the value of  $T$  is indeterminate. While this is mathematically true, there is a definite  
 98 ‘physical’ benefit in including the temperature as an additional parameter. As we discuss below, the  
 99 benefit is that of incorporating in  $T$  all the ‘collective effects’ arising in large networks, while leaving  
 100 the local properties (such as the energy of a single link) well defined in the thermodynamical limit. In  
 101 other words, if we have empirical information about the local link energies, this will fix the scale of the  
 102 problem and define the temperature unambiguously for a given network. We will indeed show examples  
 103 when, for realistic scale-free specifications of network properties, it is possible to measure the graph  
 104 temperature empirically.

## 105 2.2. Networks with finite energy per link

In general, being a combination of topological properties, the energy  $E_A$  can be an arbitrarily complicated function of the adjacency matrix  $A$ , but throughout the present paper we consider the simple and instructive case, explored in many models, where it can be written as a sum over the individual link energies  $\epsilon_{ij}$  [6,9,12]:

$$E_A \equiv \sum_{i<j} \epsilon_{ij} a_{ij} \quad (3)$$

As we show below, this choice can - despite its simplicity - give rise not only to random graphs, but also to complex scale-free networks, small-worlds, networks with correlations, clustering, and community structure. The partition function reads

$$\mathcal{Z} = \sum_{\{A\}} \prod_{i<j} e^{(\mu - \epsilon_{ij}) a_{ij}/T} = \prod_{i<j} [1 + e^{(\mu - \epsilon_{ij})/T}] \quad (4)$$

and the graph probability is

$$P_A = \prod_{i<j} p_{ij}^{a_{ij}} (1 - p_{ij})^{1-a_{ij}} \quad (5)$$

where

$$p_{ij}(T) = \frac{1}{e^{(\epsilon_{ij}-\mu)/T} + 1} \quad (6)$$

is the probability that a link between  $i$  and  $j$  exists. Equation (6) has the usual form of Fermi statistics (alternative derivations of the above expression for  $p_{ij}$  are given in refs.[6,9,20] for  $T = 1$ ). Therefore the additivity of  $E_A$  implies that each link is drawn independently with probability  $p_{ij}$ .

If the form of  $\epsilon_{ij}$  is further simplified, many important network models are obtained as particular cases of eq.(6), including hidden-variable models, the configuration model and random graphs [6]. We shall introduce the temperature-dependent version of these models in what follows. We shall also exploit eq.(6) to study a temperature-dependent small-world model, a model with community structure, and ensembles of binary graphs derived from real-world weighted networks. Therefore eq.(6) gives rise to a rich phenomenology and will be of central importance throughout the paper.

Before considering particular cases, let us first note some general properties of eq.(6). Note that, independently of  $T$ ,  $p_{ij} > 1/2$  when  $\epsilon_{ij} < \mu$  and  $p_{ij} < 1/2$  when  $\epsilon_{ij} > \mu$ . It is interesting to consider the infinite- and zero-temperature limits, as well as the ‘classical’ one.

When  $T \rightarrow +\infty$ , eq.(6) implies that

$$p_{ij}(+\infty) = \frac{1}{2} \quad (7)$$

irrespective of the values of  $\epsilon_{ij}$  and hence of the differences in the cost of links. As a consequence, the network is a random graph with  $p = 1/2$  and is therefore trivial. Note that in this case any two configurations  $A$  and  $B$  become equiprobable ( $P_A = P_B$ ).

When  $T = 0$ , we instead have

$$p_{ij}(0) = \Theta(\mu - \epsilon_{ij}) \quad (8)$$

where  $\Theta(x) = 1$  if  $x > 0$  and  $\Theta(x) = 0$  if  $x < 0$ . Technically, we should define  $\Theta(0) = 1/2$  in order to capture the correct behaviour of eq.(6), even if we will not encounter this situation in what follows. The above equation means that only those pairs of vertices for which  $\epsilon_{ij} < \mu$  are connected. This is analogous to the well-known *degenerate* behaviour of Fermions at zero temperature, and  $\mu$  is also termed the *Fermi energy*  $\epsilon_F = \mu$ . This clarifies the role of  $\mu$  as the available energy per link when  $T \rightarrow 0$ : at absolute zero, only the topology with the minimum value of  $E_A - \mu L_A$  can be realized. This topology is obtained by drawing all and only the links with  $\epsilon_{ij} < \mu$ .

A final general comment is that eq.(6) reduces to the ‘classical limit’ [6]

$$p_{ij}(T) \approx e^{(\mu-\epsilon_{ij})/T} \quad \text{when} \quad e^{(\epsilon_{ij}-\mu)/T} \gg 1 \quad (9)$$

We will consider the above limit in some applications later on.

An important consequence of the above general considerations is that, since both  $\epsilon_{ij}$  and  $\mu$  are link-specific quantities, we will be interested in the case when their value is finite and independent of the network’s size  $N$ . This is because large-scale networks arise as a bottom-up combination of local link formation processes. The energy per pair of vertices should therefore have a finite value in the thermodynamic limit ( $N \rightarrow \infty$ ). For the same reason, we will assume that  $\epsilon_{ij}$  and  $\mu$  are independent of the temperature  $T$ . In other words,  $\epsilon_{ij}$  and  $\mu$  fix the scale of pair-specific properties (that should remain

137 well-defined in the large  $N$  limit), and the collective (network-wide) effects are reabsorbed in  $T$ . As  
 138 we have anticipated above, this is the main added value of isolating  $T$  from the other parameters of the  
 139 model, and the ultimate reason why we believe that investigating the temperature dependence of network  
 140 ensembles is important. As a final remark, we require  $\epsilon_{ij}$ ,  $\mu$  and  $T$  to be dimensionless. If we imagine  
 141 that  $\epsilon_{ij}$  is (a function of) an empirically measurable quantity such as distance or money, an dimensionless  
 142 specification can be achieved by assuming that both  $\epsilon_{ij}$  and  $\mu$  have been preliminarily divided by some  
 143 appropriately averaged (either over vertices or vertex pairs) value of  $\epsilon_{ij}$ , and by simply considering  $T$  as  
 144 a dimensionless parameter. We will discuss this point in each of the following examples.

### 145 3. Random Graphs: vanishing of the percolation threshold at zero temperature

In what follows we consider various specific cases. The simplest scenario is when all link energies are equal:  $\epsilon_{ij} = \epsilon$ . This yields a temperature-dependent random graph of the Erdős-Rényi type, since all probabilities  $p_{ij}$  are equal to

$$p(T) = \frac{1}{1 + e^{(\epsilon - \mu)/T}} \quad (10)$$

146 Note that, if we assume that the  $\epsilon$  has been divided by its average value over all pairs of vertices to  
 147 make it dimensionless, we should simply set  $\epsilon = 1$ . When looking at the above formula, as well as the  
 148 following ones, this is the value of  $\epsilon$  that we should keep in mind.

While the properties of the random graph are well known, in our framework some intriguing results emerge as the temperature is varied, and in particular when  $T \rightarrow 0$ . First of all, we note that

$$p(0) = \Theta(\mu - \epsilon) \quad (11)$$

149 implying that the graph is either fully connected ( $\mu > \epsilon$ ) or empty ( $\mu < \epsilon$ ).<sup>1</sup> This result provides us with  
 150 a useful (for our purposes in what follows) definition of ‘sparseness’ of a network. We define a random  
 151 graph as *sparse* (*dense*) if  $\epsilon > \mu$  ( $\epsilon < \mu$ ), since when  $T \rightarrow 0$  the graph becomes empty (fully connected).  
 152 This means that, at finite temperature, a sparse graph (as defined above) will be such that  $p(T) < 1/2$   
 153 and a dense graph will be such that  $p(T) > 1/2$ . At infinite temperature, both sparse and dense graphs  
 154 converge to the intermediate density  $p(+\infty) = 1/2$ .

#### 155 3.1. Critical percolation temperature

Before considering other models, it is quite interesting to consider the percolation transition marking the onset of a giant connected component in an infinitely large random graph. For random graphs, it is well known that this transition occurs when the connection probability  $p$  is set to the critical value  $p_c \sim 1/N$ , i.e. when the function  $f(N)$  introduced above is  $f(N) \sim N$ . In our framework, since  $\epsilon$  and  $\mu$  are fixed, we can regard the phase transition as temperature-dependent. If  $\epsilon > \mu$  then  $p(T) > 1/2 > p_c$  at all temperatures, meaning that dense graphs are obviously always above the critical threshold. If  $\epsilon < \mu$ , there is a *critical percolation temperature*  $T_c$  such that  $p(T_c) = p_c \sim 1/N$ . Inverting, we find that for sparse graphs

$$T_c(N) \sim \frac{\epsilon - \mu}{\ln N} \quad \epsilon < \mu \quad (12)$$

<sup>1</sup>Technically, we recall that if  $\mu = \epsilon$  then  $p(0) = 1/2$ , i.e. the graph is half-connected.

In the thermodynamic limit, we have

$$\lim_{N \rightarrow \infty} T_c(N) = 0 \quad (13)$$

156 meaning that when  $N \rightarrow \infty$ , the critical percolation temperature tends to zero, i.e. the zero-temperature  
 157 topology naturally sets at the critical point  $p = p_c$ . It is well known that at this critical point the  
 158 distribution of the sizes of connected components of the network has a power law distribution of the  
 159 form  $P(s) \propto s^{-5/2}$  [1]. Interestingly, this behaviour is similar to a scenario explored in the theory of  
 160 Self-Organized Criticality (SOC), where the onset of the SOC behaviour has been related to the vanishing  
 161 of the critical temperature [21]. Combining together the above results about dense and sparse graphs,  
 162 we find that, *irrespective of their density, at finite temperature infinitely large random graphs are always*  
 163 *above the percolation threshold.*

### 164 3.2. Large and sparse graphs have low temperature

We note that the link density of most real-world socio-economic networks is (significantly) smaller than  $1/2$ . This means that, when modeled as random graphs (i.e. when considering a connection probability  $p$  equal to the observed link density  $f$ ), real networks systematically fall in the ‘sparse graph’ category and are therefore such that  $\epsilon > \mu$ . It should also be noted that in most cases the observed density typically decays as  $1/f(N)$  where  $f(N)$  is an increasing function of  $N$ . This means that, in order to reproduce the empirically observed density, random graphs should be such that

$$\frac{1}{1 + e^{(\epsilon - \mu)/T}} = \frac{1}{f(N)} \quad (14)$$

which implies

$$T = \frac{\epsilon - \mu}{\ln[f(N) - 1]} \quad (15)$$

165 This result shows that larger graphs have a smaller temperature, providing a first indication of the fact that  
 166 large real-world networks might be generally characterized by a small value of the graph temperature.

167 It is also important to note that, for most observed networks,  $f(N) \simeq cN$  with  $c \gtrsim 1$ . In combination  
 168 with eq.(12) this means that, when modeled as random graphs, large real-world networks have a low  
 169 but non-zero temperature, i.e. they are ‘just above’ the percolation threshold. This is enough to ensure  
 170 that large networks have a giant connected component. For social networks, being above the percolation  
 171 threshold ensures that, starting from any node in the giant connected component, information can diffuse  
 172 to any other node of the same component. Since in the thermodynamic limit the giant component spans  
 173 a finite fraction of an infinite network, this means that information can diffuse to a macroscopic scale.

174  
 175 Obviously, real networks are very different from random graphs. Still, the above considerations hold  
 176 true also for more realistic models of networks displaying ‘scale-free’ and ‘small-world’ properties, as  
 177 we show in the next examples. On the other hand, we also know that the way information diffuses  
 178 on real social networks is not uniquely determined by whether a giant connected component exists. In  
 179 particular, we know that information is mostly confined within denser modules, a feature that requires  
 180 the network to be partitioned into so-called ‘communities’ [4]. We will discuss this point later on, when  
 181 we will introduce a model with temperature-induced community structure.

#### 182 4. Fitness models: random graphs at high temperature, scale-free networks at low temperature

Another case of great interest is when the link energy in eq.(3) is the sum of two single-vertex contributions:

$$\epsilon_{ij} = \epsilon_i + \epsilon_j \quad (16)$$

183 For future convenience, we assume that  $\epsilon_i \leq 0 \forall i$  (this can always be achieved by an irrelevant overall  
 184 shift in the energies  $\epsilon_i \rightarrow \epsilon_i - \epsilon_{max} \leq 0$ ). Moreover, to have a dimensionless quantity we imagine that  
 185  $\epsilon_i$  (and similarly  $\epsilon_j$ ) has been preliminary divided by the absolute value of its average over all vertices.  
 186 After these operations, we therefore have  $\bar{\epsilon} = -1$  where the bar denotes an average of  $\epsilon_i$  over vertices.

The above choice leads to the graph energy

$$E_A = \sum_i \epsilon_i k_i \quad (17)$$

where  $k_i \equiv \sum_j a_{ij}$  is the degree (number of links) of vertex  $i$ . Note that all graphs  $A$  with the same degrees have the same energy  $E_A$  and are therefore equiprobable. This case therefore represents the grand-canonical version of the so-called *Configuration Model*, i.e. a model of random networks with given degrees [6]. It can also be regarded as a particular case of the class of Fitness Models [17] where each node  $i$  is characterized by a ‘fitness’ or ‘hidden variable’  $x_i$  determining the connection probability. The novelty of our approach is that the node fitness  $x_i \equiv e^{-\epsilon_i/T}$  and the ‘fugacity’  $z \equiv e^{\mu/T}$  (in terms of which the model is conveniently described [20,22]) now depend on  $T$ . We can therefore write

$$p_{ij}(T) = \frac{1}{e^{(\epsilon_i + \epsilon_j - \mu)/T} + 1} = \frac{zx_i x_j}{1 + zx_i x_j} \quad (18)$$

187 which reduces to the random graph case discussed in the previous section when all vertices have the  
 188 same value of  $\epsilon_i$  or equivalently  $x_i$ .

189  
 190 We now consider a standard procedure to obtain scale-free degree distributions, i.e. by assigning  
 191 each vertex  $i$  a fitness  $x_i$  drawn from a power-law distribution  $\rho(x) \sim x^{-\gamma}$ . It has been shown that this  
 192 choice leads to a scale-free degree distribution with the same exponent  $-\gamma$ , followed by a cut-off for  
 193 large degrees [20]. The cut-off arises from the fact that  $p_{ij}$  saturates to 1 as  $x_i \rightarrow +\infty$ , which is in turn  
 194 a reflection of the fact that the degrees cannot exceed the maximum number  $N - 1$ . Clear empirical  
 195 evidences of this saturation have been observed for instance in the analysis of the Internet [20] and of  
 196 the World Trade Web (WTW) [22].

To highlight the role of  $T$ , we now rephrase the above results in terms of the energies  $\epsilon_i$ . For convenience we introduce the non-negative quantity  $\phi_i \equiv -\epsilon_i \geq 0$ , which measures the tendency of vertex  $i$  to form connections [17]. Similarly, we define  $\phi_0 \equiv -\mu$ . Now, if we want  $x$  to be distributed according to

$$\rho(x) = (\gamma - 1)x^{-\gamma} \quad (19)$$

(where  $1 \leq x < +\infty$  and  $\gamma > 1$ ), then the quantity  $\phi_i = -\epsilon_i = T \ln x_i$  must be distributed according to

$$q(\phi) = \frac{\gamma - 1}{T} e^{-\phi(\gamma-1)/T} \quad (20)$$



197 Now, since  $\phi$  does not depend on  $T$ ,  $q(\phi)$  must be  $T$ -independent as well. The only possibility is therefore  
 198  $(\gamma - 1)/T = \lambda$  where  $\lambda$  is a constant independent of  $T$ . Note that the mean of the distribution  $q(\phi)$  is  
 199  $\bar{\phi} = \lambda^{-1}$ . On the other hand, since  $\phi_i = -\epsilon_i$  and  $\bar{\epsilon} = -1$ , we also have  $\bar{\phi} = -\bar{\epsilon} = 1$ . This means that we  
 200 must set  $\lambda = 1$ . This yields  $\gamma = 1 + T$  and

$$q(\phi) = e^{-\phi} \quad (\phi \geq 0) \quad (21)$$

$$\rho(x) = Tx^{-1-T} \quad (x \geq 1) \quad (22)$$

201 which is an important result showing how  $T$  determines  $\rho(x)$  and consequently the topology of the  
 202 network.

For instance, in the classical limit (9) we recover the  $T$ -dependent version of a model studied in  
 ref.[17]: since  $p_{ij}(T) \approx zx_i x_j$ , the expected degree  $\bar{k}_i = \sum_j p_{ij}(T) \approx zx_i \sum_j x_j$  is proportional to  $x_i$   
 and is therefore distributed as

$$P(\bar{k}) \propto \bar{k}^{-1-T} \quad (23)$$

203 In this case there are no degree correlations due to the factorization of  $p_{ij}(T)$ .

204 In the more general case (i.e. outside the ‘classical’ regime),  $P(k)$  has a power-law region with an  
 205 exponent that is still an increasing function of  $T$ , followed by a cut-off arising from the saturation of  
 206  $p_{ij}(T)$ . The power-law region narrows as  $T$  increases. This qualitative behaviour can be characterized  
 207 rigorously by computing  $\bar{k}_i$  as a function of  $x_i$  or  $\phi_i$ , and inverting this relation to find  $P(\bar{k})$  from  $\rho(x)$  or  
 208  $q(\phi)$ . This is not easy in general, but here we show that in the three paradigmatic cases  $T = +\infty$ ,  $T = 1$   
 209 and  $T = 0$  it can be done successfully.

#### 210 4.1. High-temperature regime ( $T = +\infty$ )

211 For  $T = +\infty$  we have the usual result  $p_{ij}(+\infty) = 1/2$ . So the network is a random graph with  
 212 density  $1/2$  and average degree  $N/2$ . In this regime the degree distribution  $P(\bar{k})$  approaches a trivial  
 213 Poisson distribution with mean  $N/2$ . There are no degree-degree correlations, and all nodes have an  
 214 expected clustering coefficient equal to  $1/2$ .

#### 215 4.2. Finite-temperature regime ( $T = 1$ )

216 For  $T = 1$ , denoting  $p_{ij}(T) = p(\phi_i, \phi_j)$  the expected degree of a vertex with fitness  $\phi$  can be evaluated  
 217 as the integral

$$\begin{aligned} \bar{k} &= N \int_0^{+\infty} p(\phi, \phi') q(\phi') d\phi' = N \int_0^{+\infty} \frac{q(\phi')}{e^{\phi_0 - \phi - \phi'} + 1} d\phi' \\ &= N \frac{\ln(e^{\phi_0 - \phi} + 1)}{e^{\phi_0 - \phi}} = Nzx \ln \frac{1 + zx}{zx} \end{aligned} \quad (24)$$

which is an increasing function of  $x$  and is therefore invertible. If  $x(\bar{k})$  denotes the inverse function, the  
 expected degree distribution is  $P(\bar{k}) = \rho[x(\bar{k})] dx/d\bar{k}$ . Note that  $\bar{k} \propto x$  for small  $x$ , while  $\bar{k} \rightarrow N$  for  
 large  $x$ . Thus in the linear regime (small  $\bar{k}$ ) we have  $x \propto \bar{k}$  as in the classical limit, so that  $dx/d\bar{k}$  is  
 constant and

$$P(\bar{k}) \propto \rho[x(\bar{k})] \propto \bar{k}^{-2} \quad (25)$$

218 This scale-free region is followed by a cut-off for large  $k$ , corresponding to the ‘saturated’ behaviour.

### 219 4.3. Low-temperature regime ( $T = 0$ )

Finally, when  $T = 0$  the expression for  $\rho(x)$  in eq.(22) breaks down since all the  $x_i$ ’s become infinite, and from eq.(8) we find

$$p_{ij}(0) = \Theta(\phi_i + \phi_j - \phi_0) \quad (26)$$

Surprisingly, this coincides with another model introduced in ref.[17], which precisely assumes  $q(\phi) = e^{-\phi}$  as in eq.(21) and thus turns out to be the zero-temperature limit of our general model. This model is intriguing since a derivation similar to that in eq.(24) shows that it yields a purely scale-free degree distribution

$$P(\bar{k}) = (Ne^{-\phi_0}) \bar{k}^{-2} = (Ne^\mu) \bar{k}^{-2} \quad (27)$$

(now without cut-off), even if no power-laws are introduced ‘by hand’ in the model [17,18]. Moreover, the model displays anticorrelation between degrees: the average nearest neighbour degree scales as

$$\bar{k}^{nn}(\bar{k}) \propto \bar{k}^{-1} \quad (28)$$

and the clustering coefficient scales as

$$\bar{c}(\bar{k}) \propto \bar{k}^{-2} \quad (29)$$

220 (times logarithmic corrections) [17,18].

221 We note that, while in ref. [17] the above model was proposed as an alternative way to produce  
 222 scale-free networks, different from the specification leading to eq.(23), here we find that both choices are  
 223 actually two particular cases of the same temperature-dependent model. We also note that eq.(27) cannot  
 224 be retrieved as the zero-temperature limit of eq.(23), since in such limit the ‘classical’ approximation  
 225 (9) is no longer valid. Rather, the above results show that as  $T$  goes to zero the exponent of the degree  
 226 distribution approaches  $-2$ , with a gradual disappearance of the upper cut-off. Moreover, we stress that  
 227 while the topological properties of the network depend on both the temperature  $T$  and the chemical  
 228 potential  $\mu$ , the latter strongly determines the mean of the degree distribution (i.e. the link density) but  
 229 not its functional form, which is instead mainly determined by  $T$ .

230

231 Taken together, the above results lead to the following intriguing conclusion: in this model, *correlated*  
 232 *scale-free networks with exponent  $-2$  naturally arise as the optimized topology at zero temperature. As  $T$*   
 233 *grows, the correlations become weaker, the exponent of  $P(\bar{k})$  increases and a cut-off appears destroying*  
 234 *the purely scale-free behaviour, until for  $T \rightarrow \infty$  the network becomes an uncorrelated random graph*  
 235 *with a Poisson degree distribution. In our framework, it is clear that  $\phi_0$  plays the role of a Fermi energy.*  
 236 We can also interpret the correlations at  $T = 0$  as the collective need to minimise the total energy, an  
 237 effect that gradually weakens as  $T$  increases.

### 238 4.4. The temperature of real binary networks

We now make some important considerations about the temperature of real-world binary networks. The degree distribution of most real scale-free networks has a broad tail of the form

$$P(k) \propto k^{-\gamma} \quad 2 \lesssim \gamma \lesssim 3 \quad (30)$$

The above observed range of the exponent is another remarkable indication that real networks are consistent with a low-temperature model. In particular, all binary scale-free networks in the ‘classical regime’ described by eq.(23) are consistent with a temperature

$$T_{binary} = \gamma - 1 \quad \implies \quad 1 \lesssim T_{binary} \lesssim 2 \quad (31)$$

239 Scale-free networks outside the classical regime are instead characterized by an even lower temperature,  
240 since we have shown that  $\gamma = 2$  is realized at  $T = 0$ . For these networks, a small positive value  
241  $T_{binary} > 0$  is already enough to produce a realistic degree distribution with  $\gamma > 2$ .

242 We finally note that, if one has access to the empirical distribution  $\rho(x)$ , one can measure  $T_{binary}$  for  
243 any real network which is well described by eq.(18), even if this network is not scale-free. This is for  
244 instance possible for the WTW, where  $x_i$  has been identified with the Gross Domestic Product of country  
245  $i$ , whose distribution has a fat tail consistent with a power-law with exponent  $-2$  [22]. This means that  
246  $T_{binary}^{WTW} \approx 1$  and that eq.(24) applies. This is consistent with the observed saturated behaviour of  $k(x)$   
247 and the cut-off displayed by  $P(k)$  for the real WTW [22].

## 248 5. More general models

249 One can further explore eq.(6) by considering different forms of  $q(\phi)$  and of  $\epsilon_{ij}$  as a function of  $\phi_i$   
250 and  $\phi_j$ , thus recovering the whole class of fitness models [17] with generic  $p_{ij} = p(\phi_i, \phi_j)$ . An even  
251 more general case is when  $\epsilon_{ij}$  cannot be written as a function of single-vertex contributions, so that each  
252 pair of vertices has an associated quantity  $\phi_{ij} \equiv -\epsilon_{ij}$  drawn from a distribution  $q(\phi)$ , and a probability  
253  $p_{ij} = p(\phi_{ij})$  to exist. This corresponds to the general case defined by eqs. (3) and (6).

The vanishing of the percolation threshold as shown previously in eq.(13) for the random graph example is actually a more general result, and holds even when different pairs of vertices have different values of  $\epsilon_{ij}$  as in eq.(6), i.e. when  $\epsilon_{min} \leq \epsilon_{ij} \leq \epsilon_{max} < \mu$ . In this case, we must have

$$T_{min}(N) \leq T_c(N) \leq T_{max}(N) \quad (32)$$

where

$$T_{min}(N) \equiv \frac{\epsilon_{min} - \mu}{\ln N}, \quad T_{max}(N) \equiv \frac{\epsilon_{max} - \mu}{\ln N} \quad (33)$$

From the above equations, it follows that

$$\lim_{N \rightarrow \infty} T_{min}(N) = 0, \quad \lim_{N \rightarrow \infty} T_{max}(N) = 0 \quad \implies \quad \lim_{N \rightarrow \infty} T_c(N) = 0 \quad (34)$$

254 Therefore the critical temperature vanishes in this case as well. Again, this suggests why most large  
255 social networks display a giant connected component, including the class of scale-free networks  
256 consistent with the model described above.

258 In what follows we consider three particular cases of the above model: a temperature-dependent  
 259 modification of the ‘small-world’ network model [23], a novel model of networks with community  
 260 structure, and a generalization of ensembles of binary graphs derived from weighted networks [19].  
 261 The latter allows for a direct and simple extension to real weighted networks.

## 262 6. A temperature-driven small-world model

263 The energy in eq.(6) is particularly suitable as a model of networks with geometric constraints  
 264 [15,24,25]. Indeed, if vertices represent points of a metric space, the distance between pairs of vertices  
 265 will affect the cost of a link between them. We now show that this simple fact leads to a straightforward  
 266 definition of a temperature-dependent model of small-world networks, that can be also extended to  
 267 generate networks that are both small-world and scale-free.

### 268 6.1. Non-scale-free small-worlds

In the simplest situation, the energy  $\epsilon_{ij}$  of a link is simply proportional to the distance  $d_{ij}$  between its end-point vertices. If we imagine that both  $\epsilon_{ij}$  and  $d_{ij}$  have been made dimensionless by dividing each of them by the respective average value over all pairs of vertices, the proportionality constant drops out and we can simply write

$$\epsilon_{ij} = d_{ij} \quad (35)$$

This implies

$$E_A = \sum_{i<j} \epsilon_{ij} a_{ij} = \sum_{i<j} d_{ij} a_{ij} \quad (36)$$

so that the probability of a link being there between  $i$  and  $j$  reads

$$p_{ij}(T) = \frac{1}{e^{(d_{ij}-\mu)/T} + 1} \quad (37)$$

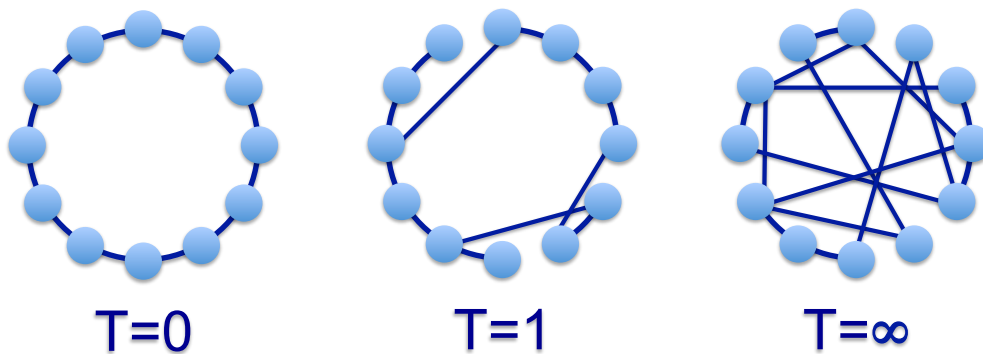
Let us first consider the zero-temperature behaviour. The above probability becomes

$$p_{ij}(0) = \Theta(\mu - d_{ij}) \quad (38)$$

269 which is nothing but the definition of a local ‘metric’ network connecting the geometrically closest  
 270 vertices (with a connectivity range set by the chemical potential  $\mu$ ). Consider for instance  $N$  vertices  
 271 equally spaced on a circle. Let  $d$  be the dimensionless distance between nearest neighbours along the  
 272 circle, i.e.  $d_{ij} = d$  if  $i$  and  $j$  are first neighbours,  $d_{ij} = 2d$  if they are second neighbours, and so on.  
 273 At zero temperature, eq.(38) implies that if  $d < \mu < 2d$  then the network is a ring with first-neighbour  
 274 interactions (as in Fig. 1), if  $2d < \mu < 3d$  then the network is a ring with second-neighbour interactions,  
 275 and in general if  $md < \mu < (m + 1)d$  (where  $m$  is a positive integer) the network is a ring with  
 276  $m$ th-neighbour interactions. If vertices are instead the nodes of a  $D$ -dimensional lattice and  $d$  is the  
 277 lattice spacing, then when  $md < \mu < (m + 1)d$  the zero-temperature network is a lattice with the same  
 278 dimensionality and with  $m$ th-neighbour interactions.<sup>2</sup>

<sup>2</sup>Note that, if we allow the chemical potential to take precisely the integer value  $\mu = md$ , then the pairs of vertices separated by a distance  $d_{ij} = md$  will be connected with probability  $p_{ij}(0) = 1/2$ , adding a sort of ‘random anomaly’ to the ring-like or lattice structure. For this reason, we have deliberately restricted  $\mu$  to take the non-integer values  $md < \mu < (m + 1)d$  so that  $\mu \neq md$ .

**Figure 1.** A temperature-dependent small-world model with vertices arranged in a circle and chemical potential  $d < \mu < 2d$  (where  $d$  is the dimensionless distance between nearest neighbours along the circle). When  $T = 0$  (left), the network is a ring with first-neighbour interactions. When  $T = \infty$  (right), the network is a random graph with connection probability  $p = 1/2$ . When  $T = 1$  (center), the network is a ‘small-world’ with a few long-range connections and an incomplete circular ‘backbone’.



279 If the temperature is slightly increased from  $T = 0$  to a small positive value, then these regular  
 280 ring-like or lattice structures will be perturbed, with a small number of short-range connections  
 281 being replaced by longer-range ones (see fig. 1). At higher temperature, the zero-temperature  
 282 structure becomes increasingly obscured and even longer-range connections are formed, until at  
 283 infinite temperature the network becomes a completely random graph with connection probability  
 284  $p_{ij}(+\infty) = 1/2$ .

285

286 From the above discussion, it is clear that this model is very similar to the popular ‘small-world’  
 287 model by Watts and Strogatz (WS) [23], where an initial lattice is perturbed by redirecting its links, with  
 288 probability  $p$ , to randomly chosen vertices. In that model, if  $p = 0$  the original lattice is preserved, if  
 289  $0 < p < 1$  part of the original lattice coexists with long-range connections or ‘shortcuts’, while if  $p = 1$   
 290 all the links are rewired as in a random graph.

291 There are two main differences between our model and the WS one. First, here for all finite values  
 292 of  $T$  longer links have a smaller probability than shorter links, whereas in the WS model distance does  
 293 not affect the probability of creating shortcuts (which is a less realistic situation). Second, here the  
 294 totally random ( $T = +\infty$ ) configuration has density  $1/2$  irrespective of the density of the initial ( $T = 0$ )  
 295 lattice, whereas in the WS model the totally random ( $p = 1$ ) configuration has the same density as the  
 296 initial ( $p = 0$ ) lattice. In fact, here the density depends monotonically on  $T$ , while in the WS model  
 297 it is independent of  $p$ . Therefore the low-temperature regime of our model is similar to the WS model  
 298 in the regime of low rewiring probability, whereas the behaviour of the two models differs in their  
 299 high-temperature/high-rewiring regimes.

300 In the limit of low rewiring probability, the standard WS model exhibits the so-called ‘small-world’  
 301 effect, i.e. the combination of a large value of the clustering coefficient (measuring the average fraction

of realized triangles at each node) and of a small value of the average vertex-vertex distance (which increases only logarithmically with the size of the graph) [1]. Since these properties are found in the low-rewiring regime, we can expect that they would be generated also in the low-temperature regime of our model. Again, this means that the empirically observed properties (in this case the small-world effect) are reproduced for small positive values of the graph temperature.

### 6.2. Scale-free small-worlds

As for the random graph model, we know that the simple small-world model (either the original WS one or our temperature-dependent reformulation above) does not reproduce the broad degree distribution so widely observed in real networks. Here, we briefly discuss how our model above can be extended in order to account for a heterogeneous - and if necessary, scale-free - degree distribution.

To this end, we combine two models considered so far, by assuming that the link energy in eq.(3) is determined not only by distances, as in the above model, but also by vertex-specific properties, as in eq.(16). This leads to

$$\epsilon_{ij} = d_{ij} + \epsilon_i + \epsilon_j \quad (39)$$

where now we imagine that  $d_{ij}$  has been divided by its average over all pairs of vertices, while  $\epsilon_i$  and  $\epsilon_j$  have been divided by their average over all vertices. Correspondingly, eq.(3) becomes

$$E_A = \sum_{i < j} d_{ij} a_{ij} + \sum_i \epsilon_i k_i \quad (40)$$

and eq.(6) becomes

$$p_{ij}(T) = \frac{1}{e^{(d_{ij} + \epsilon_i + \epsilon_j - \mu)/T} + 1} = \frac{z x_i x_j e^{-d_{ij}}}{1 + z x_i x_j e^{-d_{ij}}} \quad (41)$$

(where we have used the same definitions as in sec. 4). The above model has been recently exploited in order to study the spatial properties of the World Trade Web, where  $d_{ij}$  is the (dimensionless) geographic distance between countries  $i$  and  $j$  [15].

Clearly, a sufficiently heterogeneous distribution of the values of  $\epsilon_i$  will induce a broad degree distribution, exactly as we showed in sec. 4. In particular, a suitable choice allows to reproduce the scale-free and small-world properties simultaneously. However, a general conclusion one can learn from this model is that, if the distances arise from a homogeneous spatial distribution of vertices and if the degree distribution induced by eq.(40) is very broad, this typically means that, while the distribution of the sums  $\epsilon_i + \epsilon_j$  is very broad, the distribution of the distances  $d_{ij}$  is much more narrowly concentrated around its average value  $\bar{d} = 1$ . Looking at eq.(39), this means that the distribution of  $\epsilon_{ij}$  is mainly determined by that of  $\epsilon_i + \epsilon_j$ , i.e. we can make the approximation

$$\epsilon_{ij} \approx \bar{d} + \epsilon_i + \epsilon_j = 1 + \epsilon_i + \epsilon_j \quad (42)$$

Clearly, the constant unit term  $\bar{d} = 1$  can be reabsorbed in the chemical potential by defining  $\mu' \equiv \mu - 1$ , thus leading us back to the model defined by eq.(16) in sec. 4. For instance, when  $T = 0$  the degree distribution reads

$$P(\bar{k}) \approx (N e^{\mu-1}) \bar{k}^{-2} \quad (43)$$

316 and the degree correlations and clustering properties are still given by eqs.(28) and (29).

317

318 The above considerations mean that the scale-free property automatically implies the small-world  
319 one, whereas the converse does not hold in general. An empirical confirmation of this idea comes  
320 from the recent application of eq.(41) to the World Trade Web [15], which showed that this model  
321 only slightly improves the fit to real data with respect to the simpler model defined by eq.(18), and is  
322 in any case outperformed by other models which, instead of the distances, add to eq.(18) a different  
323 piece of information. Since for a realistically broad distribution of  $\epsilon_i$  the model reduces to the distance-  
324 independent one introduced in sec. 4, we can again conclude that the relevant range of temperature is  
325 when  $T$  is small but non-zero, exactly as in the distance-independent model. Moreover, for scale-free  
326 networks with a degree distribution given by eq.(30) the empirical value of the temperature is still given  
327 by eq.(31).

## 328 7. A model of networks with low-temperature community structure

329 We now come to a simple model of networks with community structure. To this end, we actually keep  
330 the same ingredients as in our temperature-driven small-world model defined above, with the difference  
331 that, instead of assuming that the quantities  $d_{ij}$  are metric distances among the nodes of a lattice, we  
332 imagine that they are *ultrametric* distances among the leaves of a dendrogram. In simpler words, we  
333 assume that the  $N$  vertices of the network can be categorized into a taxonomic tree with  $N$  leaves at the  
334 bottom layer, where  $d_{ij}$  is the height of the closest common branching point separating  $i$  and  $j$ .

### 335 7.1. *Ultrametric small-world model*

336 Having assumed that the distances  $d_{ij}$  are ultrametric, we further assume that the network is specified  
337 by eq.(36). The rationale for this choice is that, as an increasing body of empirical evidence suggests, the  
338 connectivity of content-rich networks such as the World Wide Web or paper citation networks is strongly  
339 determined by the semantic relationships between nodes. Web pages or scientific articles about similar  
340 topics are simply more likely to be connected to each other. Since topics are generally associated with a  
341 hierarchical taxonomy (with subcategories nested within categories), it follows that nodes with a closer  
342 common branching point in the taxonomic tree are more likely to be connected. The above qualitative  
343 properties are precisely those featured by eq.(37), having assumed an ultrametric distance  $d_{ij}$  between all  
344 pairs of vertices. We can therefore regard this model as an '*ultrametric small-world model*'. A similar  
345 idea, based on the embedding of vertices in a hyperbolic space, has been found to give rise to a rich  
346 phenomenology explaining many empirical properties of real networks [26,27].

347 Note that, since the authors of web pages or scientific articles are typically active in specialized  
348 topics, the hierarchical taxonomy will also affect the structure of social networks defined at the level of  
349 the authors themselves, e.g. networks of authors linked by coauthorship or (co-)citation. Moreover, even  
350 when  $d_{ij}$  is defined as a 'social distance' that in principle is not necessarily ultrametric (for instance,  
351 a metric distance between Euclidean vectors specifying the cultural traits of individuals), the empirical  
352 values of  $d_{ij}$  are found to be approximately ultrametric [28].

353 In this case as well, when  $T = 0$  the connection probability reduces to the deterministic expression  
 354 (38). However, the resulting network is now very different: the pairs of vertices separated by a distance  
 355 smaller than  $\mu$  are now the leaves of the dendrogram having a common branching point at a height  
 356 smaller than  $\mu$ . Equation (38) implies that all such pairs of vertices are connected, while all other pairs  
 357 are not. Visually, if we ‘cut’ the dendrogram along the horizontal direction at a height  $\mu$ , all the leaves  
 358 found within a connected branch will be the nodes of complete cliques (fully connected subgraphs) in  
 359 the network (see fig. 2a). Leaves belonging to different connected branches will not be connected, so  
 360 the network is split into as many connected components as the number of connected branches produced  
 361 by cutting the dendrogram. Higher values of  $\mu$  produce fewer and larger connected components, but at  
 362 zero temperature all such components are in any case complete cliques (see fig. 2a-b).

363 For small but positive  $T$ , the zero-temperature structure will be perturbed into a finite-temperature  
 364 one where the original cliques become ‘modules’ of densely (but not completely) connected vertices,  
 365 with a few links connecting different modules (see fig. 2c-d). This is precisely the kind of community  
 366 structure that is observed in most real socio-economic networks [4]. When  $T$  becomes large, more  
 367 missing links will be produced within communities and more links will be produced among them, until  
 368 the intra-community and inter-community densities equalize to the common value  $1/2$  in the limit  $T \rightarrow$   
 369  $+\infty$ . So, again, we find that in order to reproduce the empirical properties of socio-economic networks  
 370 (where the contrast between inter- and intra-community density is very marked, but at the same time  
 371 communities are not isolated from each other) the relevant regime of the model is the one found for  
 372 small positive  $T$ .

## 373 7.2. Ultrametric scale-free model

374 However, as for the ordinary small-world model, our ultrametric variant defined above does not  
 375 reproduce the broad degree distribution of real-world networks. But in this case as well, it is possible to  
 376 introduce the desired heterogeneity at the level of vertices by extending the model as in eqs.(39)-(41),  
 377 where now  $d_{ij}$  is an ultrametric distance. For a sufficiently high level of heterogeneity of  $\epsilon_i$ , the model  
 378 preserves the scale-free character of its distance-independent counterpart described in sec. 4. For this  
 379 reason, we call this model the ‘*ultrametric scale-free model*’.

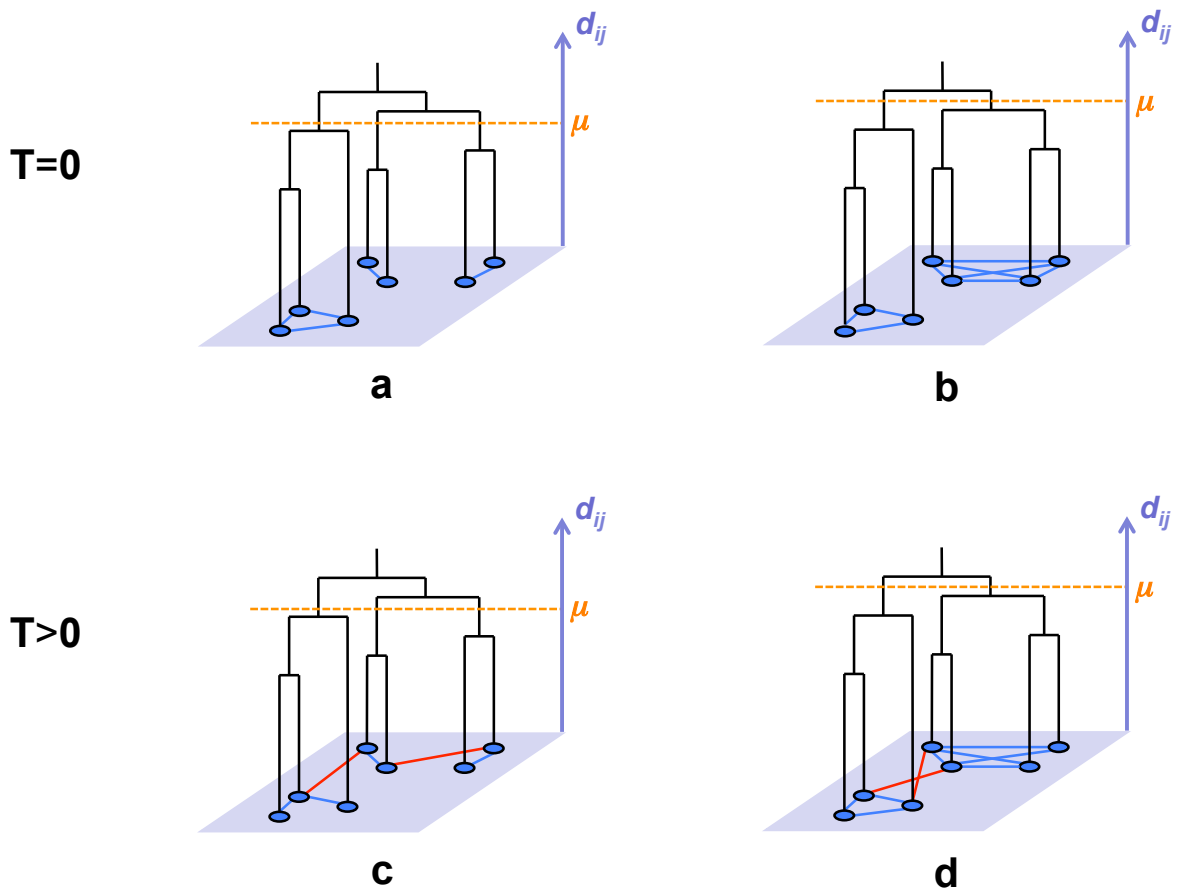
It should be noted that in this case the range of variability of  $d_{ij}$  can be much broader than in the non-ultrametric case, because here small intra-branch taxonomic distances coexist with large inter-branch ones. This means that now the approximation in eq.(42) is no longer legitimate, and we cannot reduce our model with community structure to the one without it. Rather, for all pairs of vertices  $i$  and  $j$  within the same community  $C_\mu$  (as specified by  $\mu$  when  $T = 0$ ) we now have the inequality

$$\epsilon_{ij} = d_{ij} + \epsilon_i + \epsilon_j < \mu + \epsilon_i + \epsilon_j \quad \forall i, j \in C_\mu \quad (44)$$

380 The above expression only holds within each community, while across communities the opposite  
 381 inequality applies, confirming that now distances cannot be reabsorbed in a unique value of the  
 382 chemical potential  $\mu$ . In other words, while our discussion in sec. 6 suggested that the scale-free  
 383 property automatically ensures the small-world one, here we find that the scale-free property does not  
 384 automatically ensure the presence of community structure (and vice versa). Of course, when the model  
 385 considered here displays a sufficiently heterogeneous degree distribution it will also automatically imply



**Figure 2.** Our ‘ultrametric small-world model’ as a function of temperature  $T$  and chemical potential  $\mu$ . Nodes (blue circles) are leaves of a dendrogram (black lines), separated by an ultrametric distance  $d_{ij}$  (increasing along the purple axis) representing the height of the closest branching point separating vertices  $i$  and  $j$ . The ultrametric distances determine the topology of the network (lying on the horizontal purple plane): **a**) when  $T = 0$  and  $\mu$  is small, the network is divided into many small cliques (blue links) corresponding to the disconnected branches obtained by ‘cutting’ the dendrogram along the orange dashed line determined by  $\mu$ ; **b**) when  $T = 0$  and  $\mu$  is larger, the network is divided into fewer and larger cliques; **c**) when  $T \gtrsim 0$  and  $\mu$  is small, there are many small communities that are highly connected internally (blue links) and sparsely connected across (red links); **d**) when  $T \gtrsim 0$  and  $\mu$  is larger, there are fewer and larger communities, with a higher density contrast between intra-community (blue) and inter-community (red) links. After introducing an appropriate degree of heterogeneity at the level of vertices, this model can be turned into our ‘ultrametric scale-free model’ where a non-trivial community structure coexists with a broad degree distribution.



386 the small-world property, along the lines discussed in sec. 6.

387

388 We can therefore conclude that the model defined by eqs.(39)-(41), where  $d_{ij}$  is an ultrametric  
389 distance, is a simple but highly nontrivial one. Since throughout this paper we have not been interested  
390 in reproducing a particular network, but rather a class of generic empirical properties, we will not  
391 consider any specific  $d_{ij}$  but merely note that, despite its simplicity, the above model is able to reproduce  
392 all the topological properties of real socio-economic networks discussed at the beginning: the presence  
393 of a giant connected component as ensured by eq.(34), a strong community structure induced by the  
394 ultrametric distance  $d_{ij}$ , a broad degree distribution and a small-world behaviour driven by a sufficiently  
395 heterogeneous distribution of  $\epsilon_i$  in eq.(39), and finally some realistic clustering and correlation properties  
396 as discussed in sec. 4 for the simpler model (and qualitatively preserved here). Remarkably, for each of  
397 these properties to be there, the temperature  $T$  must be small but non-zero. This summarizes why we  
398 believe that a small graph temperature might simultaneously explain a range of structural properties that  
399 are found ubiquitously in real social and economic networks.

400

401 As discussed in the Introduction, the community structure observed in real networks strongly affects  
402 the dynamics of information spreading in these systems. For most of the time, the dynamics are locally  
403 confined within communities, with occasional jumps across different communities. At a dynamical level,  
404 this implies the so-called ‘small but slow world’ effect, i.e. the fact that even if topologically short paths  
405 exist between most pairs of vertices, such paths are rarely explored dynamically unless they fall within  
406 one community.

407 The aforementioned recent study showing that the cultural distance  $d_{ij}$  among individuals of a  
408 society is effectively ultrametric [28] has also proven that this particular distribution of individuals in  
409 cultural space has dramatic effects for both short-term and long-term information dynamics. In the short  
410 term, an ultrametric distance between individuals results in the onset of a ‘coordinated’ regime where  
411 the combination of many microscopic inter-individual influences generates a society-wide collective  
412 behaviour. In the long term however, it constrains cultural convergence to the lower branches of the  
413 dendrogram, which eventually become culturally homogeneous. Taken together, these mechanisms were  
414 shown to explain the long-standing paradox of the coexistence of short-term collective social behaviour  
415 and long-term cultural diversity [28].

416 These important consequences of ultrametric distances on social and cultural dynamics suggest that  
417 our ‘ultrametric scale-free model’ promises not only to reproduce the static topology of real social  
418 networks, but to also enable a realistic simulation of distance-dependent dynamics of information  
419 diffusion.

## 420 **8. Weighted networks as temperature-dependent ensembles of binary graphs**

421 So far, we have considered binary networks. Even if, thanks to recent results characterizing various  
422 ensembles of weighted graphs [10,12,13], a full extension of our formalism to weighted networks is  
423 possible, here we only consider a simpler and practical extension that makes use of a mapping between  
424 edge weights and edge probabilities. Quite recently, we explored the idea that the empirical weights

425  $w_{ij}$  in a real weighted network can be transformed into a matrix of probabilities  $p_{ij} = p(w_{ij})$  defining  
 426 an ensemble of binary graphs [19]. Through this mapping, many topological properties which are non-  
 427 obvious for weighted networks (such as the clustering coefficient) can be re-defined as ensemble averages  
 428 of the corresponding binary quantities. In ref.[19] we explored the simplest possible choice where  $p_{ij} \propto$   
 429  $w_{ij}$ . The results presented here suggest that this choice is the ‘classical’ limit, equivalent to eq.(9), of a  
 430 more general choice that we now consider.

### 431 8.1. The temperature of real weighted networks

Turning to eq.(6), if we require  $p_{ij} = 0$  when  $w_{ij} = 0$  and  $p_{ij} = 1$  when  $w_{ij} = +\infty$ , we find that  $w_{ij}$   
 must be proportional to the *link fitness*  $e^{-\epsilon_{ij}/T}$ . In other words, the weights must depend on  $T$ , which  
 corresponds to the property that at low  $T$  (more heterogeneous weights) some pairs of vertices are much  
 more likely to be connected than other pairs, while at high  $T$  (more homogeneous weights) all pairs  
 of vertices tend to have a similar connection probability. Now, many real networks [29–33] display a  
 power-law distribution of *non-zero* link weights of the form

$$\rho(w) \propto w^{-\alpha} \quad 1.5 \lesssim \alpha \lesssim 3.5 \quad (45)$$

432 If we restrict ourselves to pairs of vertices with  $w_{ij} > 0$  and define  $x_{ij} \equiv w_{ij}/w_{min} \geq 1$  (where  $w_{min}$   
 433 is the minimum non-zero weight for a given network), corresponding to the preliminary rescaling  $\epsilon_{ij} \rightarrow$   
 434  $\epsilon_{ij} - \epsilon_{max}$ , then we can repeat the arguments leading to eq.(22). Specifically, we set  $\epsilon_{ij} \equiv -T \ln x_{ij} \leq 0$   
 435 and  $\phi_{ij} \equiv -\epsilon_{ij} \geq 0$  to obtain

$$q(\phi) = e^{-\phi} \quad (\phi \geq 0) \quad (46)$$

$$\rho(x) = T x^{-1-T} \quad (x \geq 1) \quad (47)$$

where now  $\rho(x)$  and  $q(\phi)$  are distributions not over vertices, but over pairs of them (specifically, over the  
 pairs with non-zero weights). This allows us to compute the temperature of real networks with power-law  
 distributed weights as

$$T_{weighted} = \alpha - 1 \quad \implies \quad 0.5 \lesssim T_{weighted} \lesssim 2.5 \quad (48)$$

436 The empirical values of  $\alpha$  found in various weighted networks [29–33] are summarized in Table 1, and  
 437 the corresponding values of  $T_{weighted}$  are also shown. By contrast, note that binary networks (where all  
 438 weights are equal) correspond to  $T \rightarrow \infty$  where  $x_{ij} = 1 \forall i, j$ .

439

We have therefore found that a general mapping from weights to probabilities is given by

$$p_{ij} = \frac{z x_{ij}}{1 + z x_{ij}} \quad (49)$$

where  $x_{ij} \equiv w_{ij}/w_{min}$  and  $z \equiv e^{\mu/T}$  is a free parameter. Note that the above expression works for both  
 zero and non-zero weights. We also note that the classical limit (9) of this expression reads  $p_{ij} \approx z x_{ij}$ ,  
 and if we choose  $z = w_{min}/w_{max}$  we have

$$p_{ij} \approx \frac{w_{ij}}{w_{max}} \quad (50)$$

440 which is approximately equivalent to the choice explored by us in ref.[19].

**Table 1.** Empirical values of  $\alpha$  and  $T_{weighted}$  for some real weighted networks.

Network	$\alpha$	$T_{weighted}$	Ref.
Metabolic flux networks	1.5	0.5	[29]
Interbank network	1.87	0.87	[30]
Erdős collaboration network	2	1	[31]
Chaos control & synchron. coauthorship	2.5	1.5	[31]
Financial cross-correlations	2.7	1.7	[32]
Financial cross-correlations	2.78	1.78	[33]
Financial cross-correlations	3.18	2.18	[33]
Mollusk research coauthorship	3.5	2.5	[31]
Binary graphs	$+\infty$	$+\infty$	

## 441 8.2. Filtering of weighted networks as the zero-temperature limit

442 When  $T \rightarrow 0$ , the expression (49) defining our generalized mapping from a weighted network to an  
 443 ensemble of binary graphs reduces to eq.(8). This implies that the original weighted network is mapped  
 444 into a deterministic binary one where only the links with  $\epsilon_{ij} < \mu$  are drawn. This means that the links  
 445 with weight such that  $x_{ij}(T) > z^{-1}(T)$  in the limit  $T \rightarrow 0$  are selected and the others are discarded.  
 446 Interestingly, since the ordering of the weights is preserved at all temperatures, this corresponds to  
 447 a standard thresholding procedure, adopted for instance in ref.[34] to filter stock correlations and in  
 448 ref.[35] to extract minimum spanning trees from real foodwebs. These filtering techniques discard  
 449 most of the information contained in the weights, resulting in a single (threshold-dependent) binary  
 450 graph. Here we find that this corresponds to the zero-temperature limit of our mapping from weighted  
 451 networks to ensembles of binary graphs. Our results extend these techniques to the finite temperature  
 452 case, making it possible to preserve the heterogeneity of the links and explore the whole ensemble of  
 453 possible configurations with the appropriate probabilities. We expect that this will represent an improved  
 454 filtering technique, with a significantly reduced information loss.

## 455 9. Conclusions

456 We have introduced the concept of ‘graph temperature’, which can vary from zero to infinity, in order  
 457 to explore the behaviour of networks in the limit of large network size while keeping the local properties  
 458 well-defined. Since our methodology makes use of statistical graph ensembles that extend the class of  
 459 Exponential Random Graphs widely used in social network analysis, it has a natural application as a  
 460 generalized model of social and economic networks. We showed that many structural properties that  
 461 are ubiquitous in socio-economic networks can be simply understood as the effects of an optimized  
 462 low-temperature behaviour resulting from ‘connectivity costs’, and confirmed this by measuring the  
 463 temperature of both binary and weighted real-world scale-free networks. Furthermore we have also  
 464 shown that a variety of different models and techniques can in fact be regarded as particular cases of  
 465 a more general temperature-dependent formalism. We believe that our results provide an intuitive and

466 unified understanding of many properties of real socio-economic networks, from their scale-free and  
467 small-world behaviour to their hierarchical community structure.

## 468 Acknowledgements

469 D.G. acknowledges support from the Dutch Econophysics Foundation (Stichting Econophysics,  
470 Leiden, the Netherlands) with funds from beneficiaries of Duyfken Trading Knowledge BV, Amsterdam,  
471 the Netherlands. S.E.A. acknowledges support from The Leverhulme Trust, UK and The Royal Society,  
472 UK. G.C. acknowledges support from FET project FOC (255987) and MULTIPLEX (317532).

473 **The authors declare no conflict of interest.**

## 474 References

- 475 1. Albert, R.; Barabási, A.-L. Statistical mechanics of complex networks. *Rev. Mod. Phys.* **2002**, *74*,  
476 47.
- 477 2. Newman, M.E.J. The structure and function of complex networks. *SIAM Rev.* **2003**, *45*, 167-256.
- 478 3. Granovetter, M. S. The strength of weak ties. *American journal of sociology* **1973**, 1360-1380.
- 479 4. Karsai, M.; Kivela, M.; Pan, R. K.; Kaski, K.; Kertész, J.; Barabási, A. L.; Saramaki, J. Small but  
480 slow world: How network topology and burstiness slow down spreading. *Phys. Rev. E* **2011**, *83*,  
481 025102.
- 482 5. Holland, P. W.; Leinhardt, S. An exponential family of probability distributions for directed graphs.  
483 *J. Amer. Stat. Assoc.* **1981**, *76*, 33-50.
- 484 6. Park, J.; Newman, M.E.J. Statistical mechanics of networks. *Phys. Rev. E* **2004**, *70*, 066117.
- 485 7. Berg, J.; Lässig, M. Correlated random networks. *Phys. Rev. Lett.* **2002**, *89*, 228701.
- 486 8. Burda, Z.; Jurkiewicz, J.; Krzywicki, A. Perturbing general uncorrelated networks. *Phys. Rev. E*  
487 **2004**, *69*, 026106.
- 488 9. Garlaschelli, D.; Loffredo, M.I. Multispecies grand-canonical models for networks with reciprocity.  
489 *Phys. Rev. E* **2006**, *73*, 015101(R).
- 490 10. Garlaschelli, D.; Loffredo, M. I. Generalized bose-fermi statistics and structural correlations in  
491 weighted networks. *Phys. Rev. Lett.* **2009**, *102*, 038701.
- 492 11. Bianconi, G. Entropy of network ensembles *Phys. Rev. E* **2009**, *79*, 036114.
- 493 12. Squartini, T.; Garlaschelli, D. Analytical maximum-likelihood method to detect patterns in real  
494 networks. *New Journal of Physics* **2011**, *13*, 083001.
- 495 13. Squartini, T.; Picciolo, F.; Ruzzenenti, F.; Garlaschelli, D. Reciprocity of weighted networks.  
496 *arXiv:1208.4208*.
- 497 14. Squartini, T.; Garlaschelli, D. Triadic motifs and dyadic self-organization in the World Trade  
498 Network. In *Self-Organizing Systems*; Kuipers, F.A.; Heegaard, P.E., Eds.; Springer: Berlin  
499 Heidelberg, 2012; pp. 24-35.
- 500 15. Picciolo, F.; Ruzzenenti, F.; Basosi, R.; Squartini, T.; Garlaschelli, D., The Role of Distances in the  
501 World Trade Web, *Eighth International Conference on Signal Image Technology and Internet Based  
502 Systems (SITIS)* **2012**, 784-792.

- 503 16. Newman, M.E.J.; Strogatz, S.H.; Watts, D.J. Random graphs with arbitrary degree distributions and  
504 their applications. *Phys. Rev. E* **2001**, *64*, 026118.
- 505 17. Caldarelli, G.; Capocci, A.; De Los Rios, P.; Muñoz, M.A. Scale-free networks from varying vertex  
506 intrinsic fitness. *Phys. Rev. Lett.* **2002**, *89*, 258702.
- 507 18. Boguñá, M.; Pastor-Satorras, R. Class of correlated random networks with hidden variables. *Phys.*  
508 *Rev. E* **2003**, *68*, 036112.
- 509 19. Ahnert, S.E.; Garlaschelli, D.; Fink, T.M.; Caldarelli, G. Ensemble approach to the analysis of  
510 weighted networks. *Phys. Rev. E* **2007**, *76*, 016101.
- 511 20. Park, J.; Newman, M.E.J. Origin of degree correlations in the Internet and other networks. *Phys.*  
512 *Rev. E* **2003**, *68*, 026112.
- 513 21. Gabrielli, A.; Caldarelli, G.; Pietronero, L. Invasion percolation with temperature and the nature of  
514 self-organized criticality in real systems. *Phys. Rev. E* **2000**, *62*, 7638.
- 515 22. Garlaschelli, D.; Loffredo, M.I. Fitness-dependent topological properties of the world trade web.  
516 *Phys. Rev. Lett.* **2004**, *93*, 188701.
- 517 23. Watts, D.J.; Strogatz, S.H. Collective dynamics of small-world networks. *Nature* **1998**, *393*, 440-  
518 442.
- 519 24. Barthélemy, M. Spatial networks. *Physics Reports* **2011**, *499*, 1-101.
- 520 25. Ruzzenenti, F.; Picciolo, F.; Basosi, R.; Garlaschelli, D. Spatial effects in real networks: Measures,  
521 null models, and applications. *Phys. Rev. E* **2012**, *86*, 066110.
- 522 26. Krioukov, D.; Papadopoulos, F.; Vahdat, A.; Boguna, M. Curvature and Temperature of Complex  
523 Networks. *Phys. Rev. E* **2009**, *80*, 035101(R).
- 524 27. Krioukov, D.; Papadopoulos, F.; Kitsak, M.; Vahdat, A.; Boguna, M. Hyperbolic Geometry of  
525 Complex Networks. *Phys. Rev. E* **2010**, *82*, 036106.
- 526 28. Valori, L.; Picciolo, F.; Allansdottir, A.; Garlaschelli, D. Reconciling long-term cultural diversity  
527 and short-term collective social behavior. *Proceedings of the National Academy of Sciences* **2012**,  
528 *109*, 1068-1073.
- 529 29. Almaas, E.; Kovács, B.; Vicsek, T.; Oltvai, Z.N.; Barabási, A.-L. Global organization of metabolic  
530 fluxes in the bacterium *Escherichia coli*. *Nature* **2004**, *427*, 839-843.
- 531 30. Boss, M.; Elsinger, H.; Summer, M.; Thurner, S. Network topology of the interbank market.  
532 *Quantitative Finance* **2004**, *4*, 677-684.
- 533 31. Li, C.; Chen, G. Network connection strengths: Another power-law? *cond-mat/0311333*.
- 534 32. Kim, H.-J.; Lee, Y.; Kahng, B.; Kim, I.-M. Weighted scale-free network in financial correlations.  
535 *Journal of the Physical Society of Japan* **2002**, *71*, 2133-2136.
- 536 33. Burda, Z.; Jurkiewicz, J.; Nowak, M.A.; Papp, G.; Zahed, I. Levy Matrices and Financial  
537 Covariances. *Acta Physica Polonica B* **2003**, *34*, 4747-4763.
- 538 34. Onnela, J.-P.; Kaski, K.; Kertesz, J. Clustering and information in correlation based financial  
539 networks. *Eur. Phys. J. B* **2004**, *38*, 353-362.
- 540 35. Garlaschelli, D.; Caldarelli, G.; Pietronero, L. Universal scaling relations in food webs. *Nature*  
541 **2003**, *423*, 165-168.

542 © September 8, 2021 by the authors; submitted to *Entropy* for possible open access  
543 publication under the terms and conditions of the Creative Commons Attribution license  
544 <http://creativecommons.org/licenses/by/3.0/>.